JOURNAL OF MATERIALS SCIENCE 20 (1985) 1571–1585

Solution crystallization of polyethylene at high temperatures

Part 1 *Lateral crystal habits*

S. J. ORGAN, A. KELLER
H. H. Wills Physics Laboratory, University of Bristol, Tyndall Avenue, Bristol, UK

Polyethylene single crystals have been grown from solution in a variety of solvents at temperatures up to 120° C. Thus an overlap is achieved with conditions used for melt growth in terms of both absolute crystallization temperature (T_c) and supercooling (ΔT). Interesting developments in two-dimensional crystal habits, including the increase in axial ratio and curvature of lateral crystal faces (lamellar prism faces), have been examined and quantified. The crystal habit is found to depend primarily on T_c, regardless of solvent, although some ΔT dependence is indicated within a series of similar solvents. As T_c is raised the {100} crystal faces become increasingly curved and the {110} faces also begin to exhibit a slight curvature. The implications of these morphological developments for theories of polymer crystallization are discussed and the justification of new approaches embodying also the lateral habit features, at least in the extended T_c ranges considered here, is indicated. Also, similarities with crystals grown under similar conditions from the melt are noted.

1. Introduction

Five interrelated papers on the subject of polymer crystallization, as exemplified by polyethylene, are being submitted simultaneously. The first three form a three-part series dealing with crystallization from solution (this paper, [1, 2]). The fourth paper [3] deals with a particular aspect of melt crystallization pertinent to issues being pursued in this laboratory, as does the fifth [4] with the important addition of creating a unifying basis for both solution and melt crystallization by drawing on the full material presented by the five papers.

2. Background and purpose

Polyethylene single crystals grown from solution, the subject of the present three part series, has been widely studied in the past [5] and the technical and conceptual methods are correspondingly well-established. The work presented here attemps to fill a long-outstanding gap in the field and has wider implications for the understanding of polymer crystallization, which will be outlined below.

Work on polyethylene crystals has developed traditionally along two lines: solution and melt crystallization. Isolated single crystals grown from solution provided the basis for an academic inquiry into the nature of polymer crystallization, which led to the discovery of chain folding and other unique structural features. The first theoretical models of polymer crystal growth were based on these results. Solution crystallization was nevertheless regarded as a special case, since the vast majority of practical applications involved polyethylene solidified from the melt. Since the early recognition of chain folded lamellae in solution, most attention, even in fundamental issues, has shifted to the melt case. It is clear that any complete understanding of polymer crystallization must encompass both extremes of behaviour, but attempts to draw comparisons between the two reveal major gaps in our knowledge.

The prevailing theories of polymer crystal growth [6] were originally developed to account for chain folding and variations in fold length (as manifest by lamellar thickness) seen in single crystals. They predict that the fold length should be

0022–2461/85 $03.00 + .12

uniquely determined by the supercooling at which a crystal is grown. In practice it is found that fold lengths are very much higher for melt crystallized material than for crystals grown from solution, both in absolute terms and as related to equivalent supercooling. This apparent contradiction is resolved by the recognition of isothermal thickening, a process by which crystals may thicken by refolding during growth [7]. The final crystal thickness cannot therefore be taken as a measure of the primary fold length (l_g^*) predicted by theory. Isothermal thickening is well documented in melt crystallization and in this case verification of the theories has rested on lateral growth rate data alone. For solution crystallization, the possiblity of isothermal thickening was not originally suspected and such crystals have been assumed to be free from the effect. However, in the light of subsequent experience with the melt this assumption no longer seems assured. If thickening does occur during solution growth then the very foundation of our present ideas on these systems is threatened. In fact there is one more recent approach which explicitly challenges the traditional view by invoking isothermal thickening as being responsible for the observed fold length variations in solution-grown crystals [8].

The above uncertainties set the scene for our renewed activities on the crystallization of polyethylene. The general objective was to bridge the gap between melt and solution crystallization. More specifically, the aims were: (1) to determine the primary fold length (l_g^*) in melt crystallization by eliminating or separating the contribution of isothermal thickening and (2) to assure ourselves that isothermal thickening is indeed absent in the case of solution crystallization as has hitherto been assumed or alternatively, to find out when it occurs and assess the magnitude of the effect. (1) has been the subject of a three-part series entitled "New Look at the Crystallization of Polyethylene" [9–11]. The paper to follow the present three-part series [3] will extend and to some extent revise these previous results on crystallization from the melt. The parallel studies to all of those above, as applied to solution crystallization, (2) above, form the subject of the present series.

To facilitate comparison between solution and melt growth we require an overlap in crystallization conditions in terms of both supercooling (ΔT) and absolute temperature (T_c). Experimentally, this necessitated a lowering of the accessible range of T_c for the melt and a raising of T_c for the solution. The former has been achieved previously [11]. The attainment of the latter is described in the present series and some of the consequences will be considered.

One important aspect of the work concerns the fold length values, which will be treated in Part 3 with due scrutiny for isothermal thickening [2]. As will be apparent by combining these results with those on melt crystallization [3] complete overlap of l_g^* values for melt and solution crystallization has been achieved over a wide range of supercoolings [4]. This is in accordance with the general guiding hypothesis expressed by Barham *et al.* [9] that l_g^* is determined primarily by supercooling, while isothermal thickening depends largely on the absolute temperature.

In addition to the fold length measurements, interesting developments in crystal habits which occur as the crystallization temperature is raised have been studied. Crystal habit has never been a central issue in polymer science, but deserves attention, both as one (particularly interesting) example of crystal growth in general and also as a reflection of the mechanism of crystal growth. The external lateral habit of a crystal and its internal structure are, in a general sense, closely linked. In the simplest case, folding along prism faces produces faceted crystals which exhibit internal sectorization, with numerous consequences. The changes in internal structure as the crystal habits become less well-defined is the subject of Part 2 of this series [1], which considers diffraction and melting behaviour of crystals grown at high crystallization temperatures (T_c).

As the crystallization temperature is raised, changes occur in the nature and ratio of the crystallographic prism faces. At the same time a qualitatively new habit feature emerges as faces begin to exhibit various degrees of curvature. The effect has been observed previously [12, 13], but the profound implications of these rounded facets have never been fully explored. Curvature on the macroscopic scale implies a molecularly rough surface which seems irreconcilable with the present models of polymer crystal growth. The currently accepted kinetic theory involves the nucleation and growth of chain folded strips along crystallographic surfaces, which are either smooth or contain occasional kinks or niches without affecting the overall crystallographic direction of the face.

The existence of curved faces provides a challenge to this model and has initiated a new approach to the molecular theory of polymer crystal growth based on equilibrium surface roughness [14]. This new approach, while not replacing the traditional model, offers to extend our existing conceptions of the molecular basis of polymer crystallization in the regime of high temperature growth. Study of the onset and development of curvature in single crystals is the subject of the present paper, and as it will emerge, the curvature is found to be related to the absolute temperature of growth. Curved facets are also observed in material crystallized from the melt under similar conditions. It follows, therefore, that the study of lateral habits is of more than peripheral interest: it promises to extend our existing understanding of polymer crystal growth and to aid in the linking up of solution and melt growth. This paper, Part 1 of the series, provides documentation for both these purposes by presenting quantitative measurements of crystal habits using a wide range of crystallization conditions.

3. On the lateral crystal habits

The lamellar nature of polyethylene single crystals grown from dilute solution is well known. Extensive studies have been carried out on such crystals grown at temperatures below about 95° C e.g. [15, 16], and they are known to exhibit well-defined fold lengths and habits characteristic of the conditions of growth. Typical habits are shown in Fig. 1; as seen they closely reflect the symmetry of the unit cell. Crystals are bounded by four {1 1 0} faces, with truncating {1 0 0} faces appearing as the concentration or crystallization temperature is raised. By using poorer solvents it is possible to extend the upper limit of crystallization temperature, whereupon further developments in morphology can be seen.

The major previous studies of this type have been those of Keith [12] and Khoury and Bolz [13]. Keith crystallized low and high molecular weight fractions of polyethylene at temperatures up to 110° C from thin films, using n-alkanes (mainly n-$C_{32}H_{66}$) as solvents. He found that the axial ratio of the crystals increased with crystallization temperature and with concentration, crystals becoming more elongated in the *b* direction. Crystals grown from low molecular weight polymer tended to have higher axial ratios than those grown under the same conditions from high molecular weight material. Keith also obtained radially arranged aggregates of crystals and compared these structures to the radial crystalline units in melt grown spherulites. Khoury and Boltz, using mainly dodecanol and heptyl acetate as solvents to grow crystals at temperatures up to 120° C, confirm the findings of Keith with respect to crystallization temperature, concentration and molecular weight. They also point out the increasing curvature of the nominally {1 0 0} faces as the axial ratio increases, and the effect of solvent. For a given crystallization temperature and molecular weight, the axial ratio was larger for crystals grown from heptyl acetate than dodecanol, which is a poorer solvent. Crystals have also been grown by Nakajima *et al.* [17] at temperatures up to 109° C using various solvents, and their thicknesses measured, but the corresponding crystal morphologies were not studied.

The purpose of the present work is to obtain a broad base of quantitative data relating the lateral crystal habit to crystallization temperature in a variety of solvents, using a constant solution concentration and molecular weight distribution. Possible correlations between these lateral crystal habits and other properties such as supercooling, degree of sectorization and the associated three

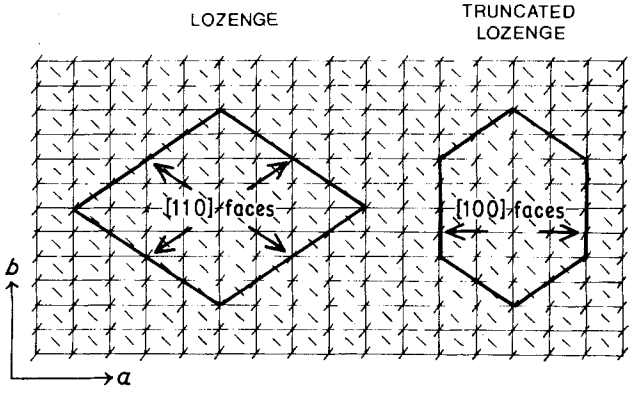

Figure 1 Typical morphologies of polyethylene single crystals and their relationship to the unit cell.

dimensional morphology [1] and crystal fold length [2] can then be examined, also in relation to the different theories of polymer crystallization as to be pursued in Part 2 [1] and Part 3 [2].

4. Experimental procedure

Conventional crystallization methods were used. In all cases the polymer was Rigidex 50, a commercial linear polyethylene supplied by BP with $M_w \simeq 100\,000$ and $M_w/M_n \simeq 10$. The lowest molecular weights were removed by a preliminary crystallization at 70° C in xylene, followed by filtration at that temperature to remove uncrystallized material. The remaining polymer was thoroughly washed and dried and used for all subsequent preparations.

Crystals were grown from 0.05% w/v solution. The solvents used were xylene, the paraffins n-octane (C_8H_{18}), n-dodecane ($C_{12}H_{26}$), n-hexadecane ($C_{16}H_{34}$), n-tetracosane ($C_{24}H_{50}$) and n-hexatriacontane ($C_{36}H_{74}$), ethyl esters ranging from ethyl caproate ($CH_3(CH_2)_4CO_2C_2H_5$) to ethyl laurate ($CH_3(CH_2)_{10}CO_2C_2H_5$), hexyl acetate ($CH_3CO_2C_6H_{13}$) and the aliphatic alcohols dodecanol ($CH_3(CH_2)_{11}OH$) and tetradecanol ($CH_3(CH_2)_{13}OH$). This choice of solvents permitted crystallization over the temperature range 70 to 120° C. In all preparations the self-seeding technique [18] was employed to produce uniform, regular crystals. Suitable seeding temperatures, T_s, which would give crystals with lateral dimensions of a few microns had been determined previously for each solvent. The crystallization and specimen preparation followed well established lines. Nevertheless, as this has never been placed on record adequately for exact reproduction a brief description is included here. The basic crystallization apparatus is shown in Fig. 2. A pre-crystallized crystal suspension is put into the left-hand chamber of the vessel, heated to T_s in an oil bath at about 10° C h^{-1}, and held at T_s for ten min. The vessel is then transferred to another oil bath at the crystallization temperature, T_c, and the solution left for three days to crystallize.

The accessible T_c range is determined by the crystallization rates. The upper limit is the highest temperature at which a readily detectable amount of polymer will crystallize within three days. The lower limit is restricted by the fact that the solution will take some time to cool to the required crystallization temperature, and at moderate to high supercoolings the rate of crystallization will be such

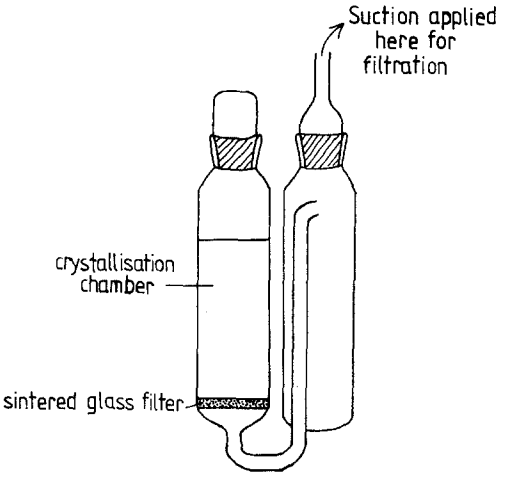

Figure 2 Crystallization apparatus.

that considerable material may crystallize during the cooling process. To determine the maximum supercooling which could confidently be attained using this method, a preliminary experiment was carried out for each solvent. A suspension of crystals was allowed to cool from T_s in an oil bath at a lower temperature and the temperature at which a noticeable amount of material (about 20%) had precipitated out was noted. The minimum crystallization temperature used was at least 5° C above this point. After three days, each crystal suspension was filtered at T_c by applying suction (see Fig. 2) to remove about 95% of the solvent. (It is necessary to leave a small amount of solvent to prevent the crystals from sticking together). The remaining slurry was then quenched by adding solvent at room temperature, so that any polymer still remaining in solution would crystallize at a much lower temperature and be easily distinguishable from the major portion of the material which had crystallized isothermally. In some cases the filtered crystals were washed with more solvent at T_c and re-filtered, to further reduce the effects of uncrystallized material. Crystals were prepared for microscopy by washing with fresh distilled solvent, and exchanging the less volatile solvents for xylene. Each preparation was first examined in a Zeiss phase-contrast optical microscope to obtain an overall view of the size, shape and distribution of the crystals. Suitable preparations, i.e. those consisting of small, well-dispersed crystals with little overgrowth, were prepared for transmission electron microscopy (TEM).

A Philips 301 transmission electron microscope operating at 100 kV was used for observation. Exposure of polyethylene crystals to an electron

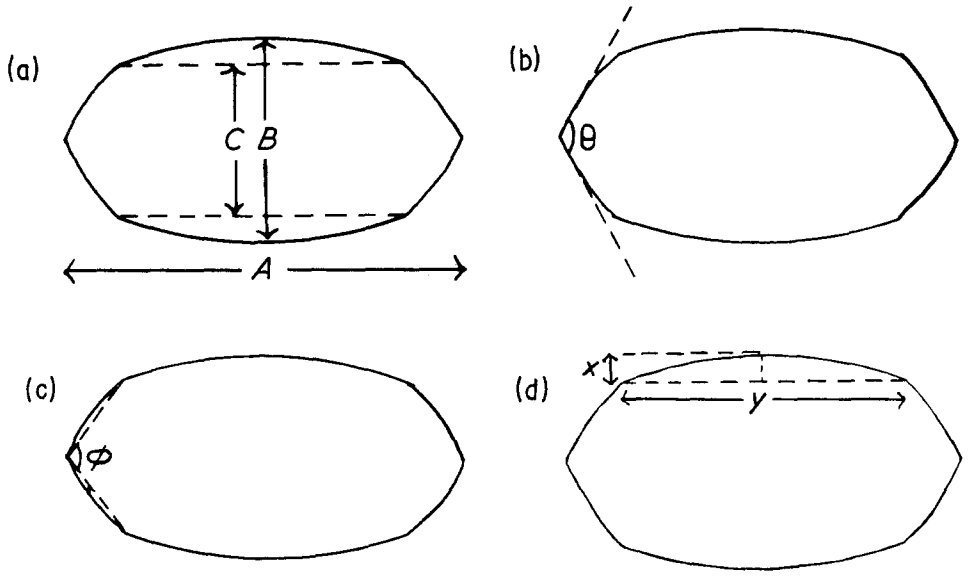

Figure 3 Parameters used for characterizing the crystal habits: (a) The minimum and maximum axial ratios, A/B and A/C, respectively. (b) The apex angle, θ. (c) The angle between the apex and the point of intersection of the "1 0 0" with the "1 1 0" faces, ϕ. (d) The curvature of the "1 0 0" faces, x/y.

beam causes changes in the lattice structure of the crystals, mainly due to cross-linking [19]. Although this beam damage affects chain tilts within the crystals, their two-dimensional shapes are not seriously altered when on a carbon substrate since this constrains the expansion which would otherwise occur [20].

5. Characterization of the crystal habits

It is common and convenient to discuss crystal habits in terms of the {1 1 0} and {1 0 0} faces, as illustrated in Fig. 1. However, as these faces become more curved, they deviate substantially from the exact crystallographic directions. Throughout this paper, the notation "1 1 0" and "1 0 0" is used to represent nominal {1 1 0} and nominal {1 0 0} faces, respectively.

To enable quantitative comparisions of crystal morphologies the following parameters were measured.

1. The minimum and maximum axial ratios, A/B and A/C, as defined in Fig. 3a.

2. The apex angle, θ, at the intersection of the "1 1 0" faces, as shown in Fig. 3b.

3. The angle between the apex and the point of intersection of the "1 0 0" with the "1 1 0" faces, ϕ, as shown in Fig. 3c.

4. The curvature of the "1 0 0" faces, expressed as the ratio x/y, where x and y are as shown in Fig. 3d.

These parameters were measured from enlarged electron micrographs of typically 15–20 crystals from each preparation studied. Average values were calculated and used to construct a representative "typical crystal" for each case. It should be pointed out that the "typical crystal" is, in fact, a rather idealized entity. Many of the actual crystals will deviate in various ways from the ideal, and some common imperfections will be described later. In calculating average values for the parameters, only the most regular crystals from each preparation were used. However, in most samples crystals which are highly regular form a large enough proportion of the whole population to be considered representative. Although the method involves some oversimplification, it provides a useful means of comparison between the crystals.

The shape of a crystal depends on the relative growth rates of its different surfaces. During growth the high index faces advance rapidly and disappear, and the slow growing, usually close-packed, faces determine the overall growth rate and shape of the crystal. A useful construction for representing the relative growth rates associated with particular habits is the "slowness diagram", as described by Frank [21]. This is a polar diagram showing the

TABLE I Range of seeding temperatures T_s, and crystallization temperatures T_c, used in the experiments

Type of solvent	Solvent	Formula	T_s range (° C)	T_c range (° C)
	Xylene	$C_6H_4(CH_3)_2$	101–102	78–95
Paraffins	Octane	C_8H_{18}	109–110	85–100
	Dodecane	$C_{12}H_{26}$	111–112	87–106
	Hexadecane	$C_{16}H_{34}$	115–116	89–108
	Tetracosane	$C_{24}H_{50}$	121–122	98–114
	Hexatriacontaine	$C_{36}H_{74}$	123–124	102–116
Esters	Hexyl acetate	$CH_3CO_2C_6H_{13}$	119–120	100–112
	Ethyl esters	$CH_3(CH_2)_4CO_2C_2H_5$ to $CH_3(CH_2)_{10}CO_2C_2H_5$	120–121	100–112
Alcohols	1-Dodecanol	$CH_3(CH_2)_{11}OH$	126–127	105–120
	1-Tetradecanol	$CH_3(CH_2)_{13}OH$	125–126	104–118

reciprocal of the growth velocity (defined as measured normal to the actual surface of the crystal) as a function of orientation. For a crystal with straight edges the slowness diagram will show "spikes" at angles normal to the directions of the faces. If the edges are curved the spikes will be replaced by "lobes" showing the angular dependence of the growth rates. The relative growth rates of different crystal surfaces can be easily seen from the relative lengths of these lobes.

6. Results

Table I gives the range of seeding temperatures and crystallization temperatures used for each solvent. Fig. 4 shows a selection of electron micrographs which illustrate the different crystal morphologies obtained as the solvent and crystallization temperature are varied. A general trend towards higher axial ratios and increased curvature can be seen as the crystallization temperature is raised. Before analysing these transitions in crystal shape more quantitatively, it is interesting to note several other features which are illustrated in the micrographs.

1. The self-seeding technique ensures that the crystals are small and regular. In some cases, for instance Figs. 4i and j the seeds are visible as small protrusions in the centre of the crystals. Many of the crystals are monolayers, but all preparations also contained some multilayers. Multilayer growth occurs through screw dislocations, which lead to growth spirals with their axes along the chain direction. Good examples are seen in Figs. 4a and c. The extra layers usually grow in the same shape and orientation as the base of the crystal.

2. Signs of collapse are common. Almost all the sedimented crystals show pleats, evidence of the

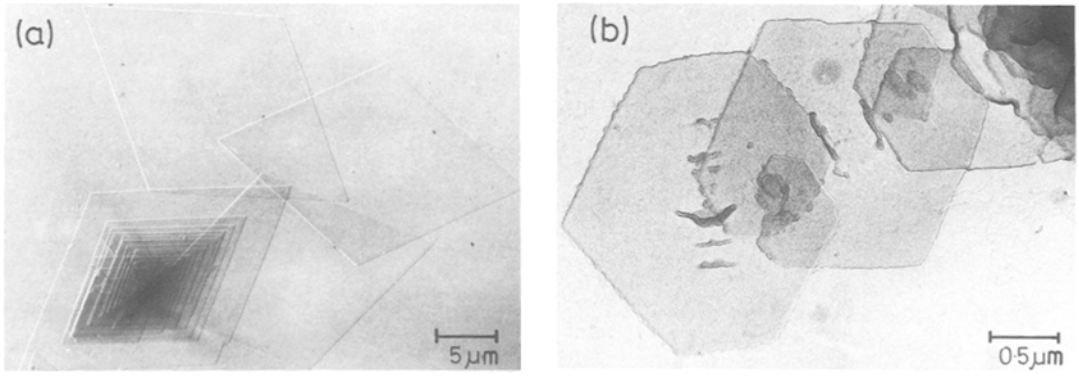

Figure 4 Electron micrographs showing single crystals of polyethylene grown from 0.05% solution in the solvents, and at the crystallization temperatures, shown. All except (c), (f) and (h) are shadowed with Pt–Pd. (a) Xylene $T_c < 70°$ C, (b) xylene $T_c = 86.0°$ C, (c) octane $T_c = 93.0°$ C, (d) xylene $T_c = 94.0°$ C, (e) hexadecane $T_c = 96.5°$ C, (f) dodecane $T_c = 98.8°$ C, (g) hexadecane $T_c = 103.1°$ C, (h) hexatricontane $T_c = 105.6°$ C, (i) ethyl ester $T_c = 107.0°$ C, (j) tetradecanol $T_c = 107.8°$ C, (k) ethyl ester $T_c = 111.8°$ C, (l) tetradecanol $T_c = 111.8°$ C, (m) hexatriacontane $T_c = 112.8°$ C, (n) hexatriacontane $T_c = 115.0°$ C.

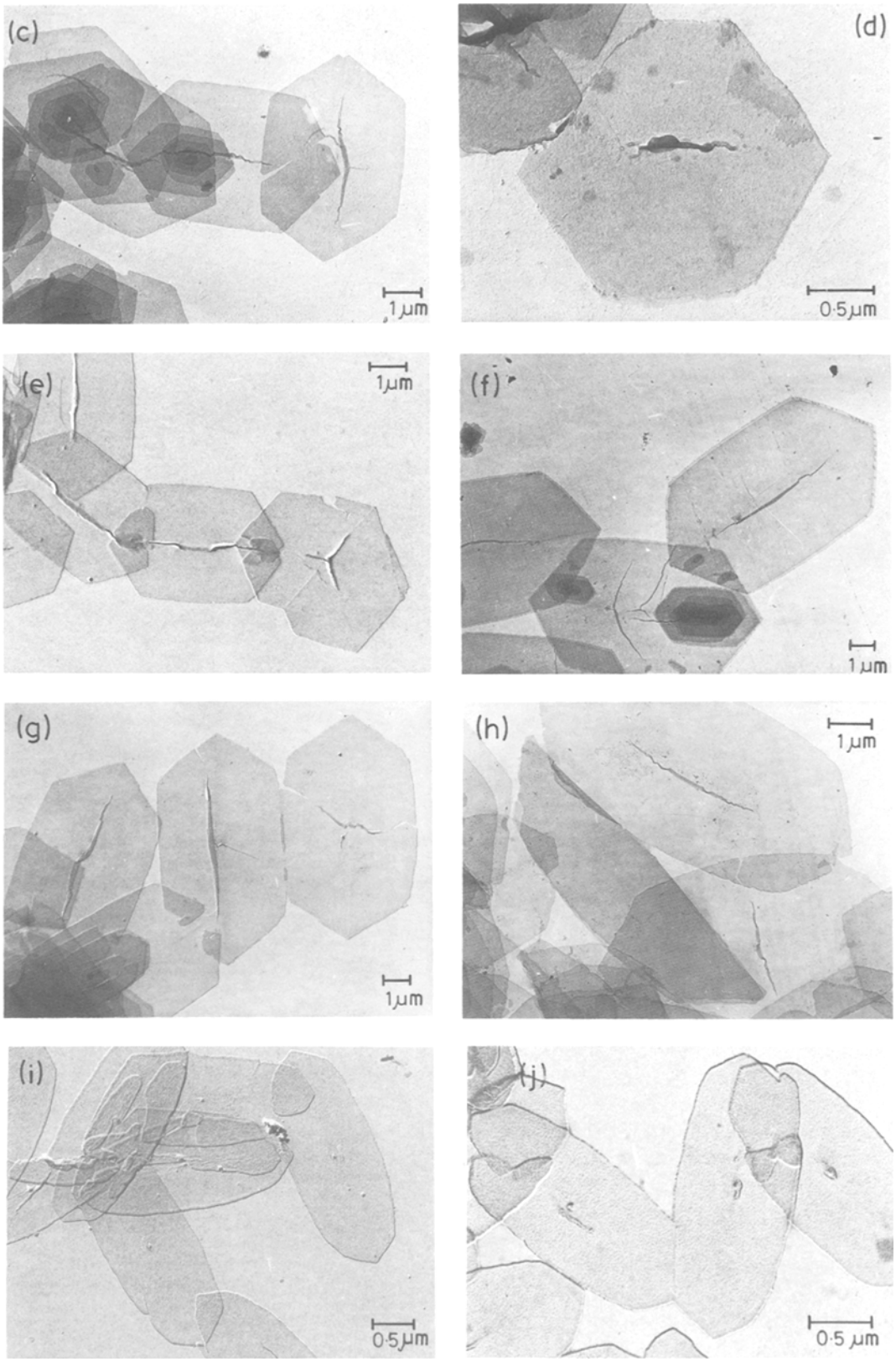

Figure 4 Continued.

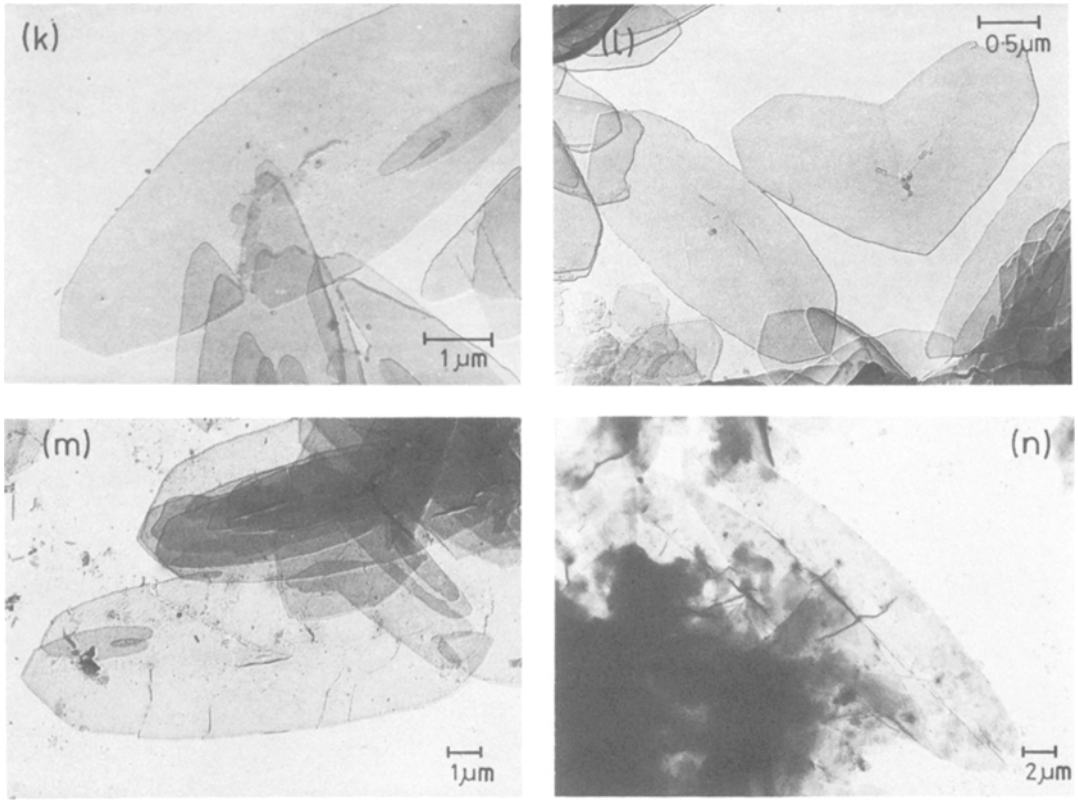

Figure 4 Continued.

original three-dimensional structure, and some also have tears. In addition in Fig. 4m pulled fibrils, roughly parallel to the crystal edge, can be seen. All these features are familiar consequences of sectorization and require no further comment.

3. Examples of both "Siamese twins" and "growth twins" (as defined by Blundell and Keller [22]), are occasionally seen. Siamese twins result from the joining of two or more crystals during growth, and some can be seen in Fig. 4g. In the case of growth twins, two twin components grow from a common centre lying on the twin boundary—usually (1 1 0) or (3 1 0). They are thought to arise from a multi-componenet nucleus, possibly consisting of two separate nuclei joined together by loose chains. Figs. 4e and 1 show examples of (1 1 0) growth twins.

4. Crystals grown at the higher temperatures or from particular solvents (notably hexyl acetate and dodecanol) tended to grow in complex clusters or in a highly multilayered form, as illustrated in Fig. 5. The original three-dimensional structure of the clusters is difficult to infer from their dried-down forms but they would appear to consist of many crystals, growing from a common centre in all directions. Twisting of crystals is suggested in some cases. Some preparations contained both monolayers and clusters which showed similar underlying morphology. Both the dimensions of the clusters and the limited morphological information available from the electron micrographs suggest that the crystals are connected at their centres. This is in contrast to the radiating aggregates of crystals obtained by Keith [12] where the crystals appear to be joined at their apices. The clusters show some similarities with spherulitic growth.

Fig. 6 shows a selection of "typical crystal" habits, together with their slowness diagrams. The slowness diagrams are arbitrarily normalized to a common "1 1 0" face growth rate. Table II lists the values of the parameters corresponding to these habits and also gives the ratio of the growth rates of the "1 1 0" and "1 0 0" faces, G_{110}/G_{100}. The growth rates are assumed to be proportional to the perpendicular distance from the centre of a crystal to a tangent at the mid-point of the crystal edge.

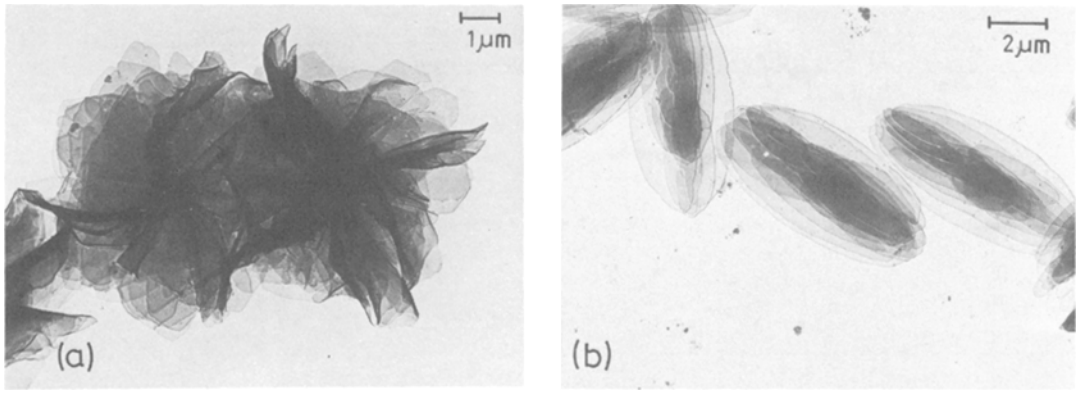

Figure 5 Electron micrographs of polyethylene crystals. (a) Grown from hexyl acetate at 102.9° C and showing cluster morphology. (b) Grown from tetradecanol at 118.0° C and showing highly multilayered structure. (b) is shadowed with Pt–Pd.

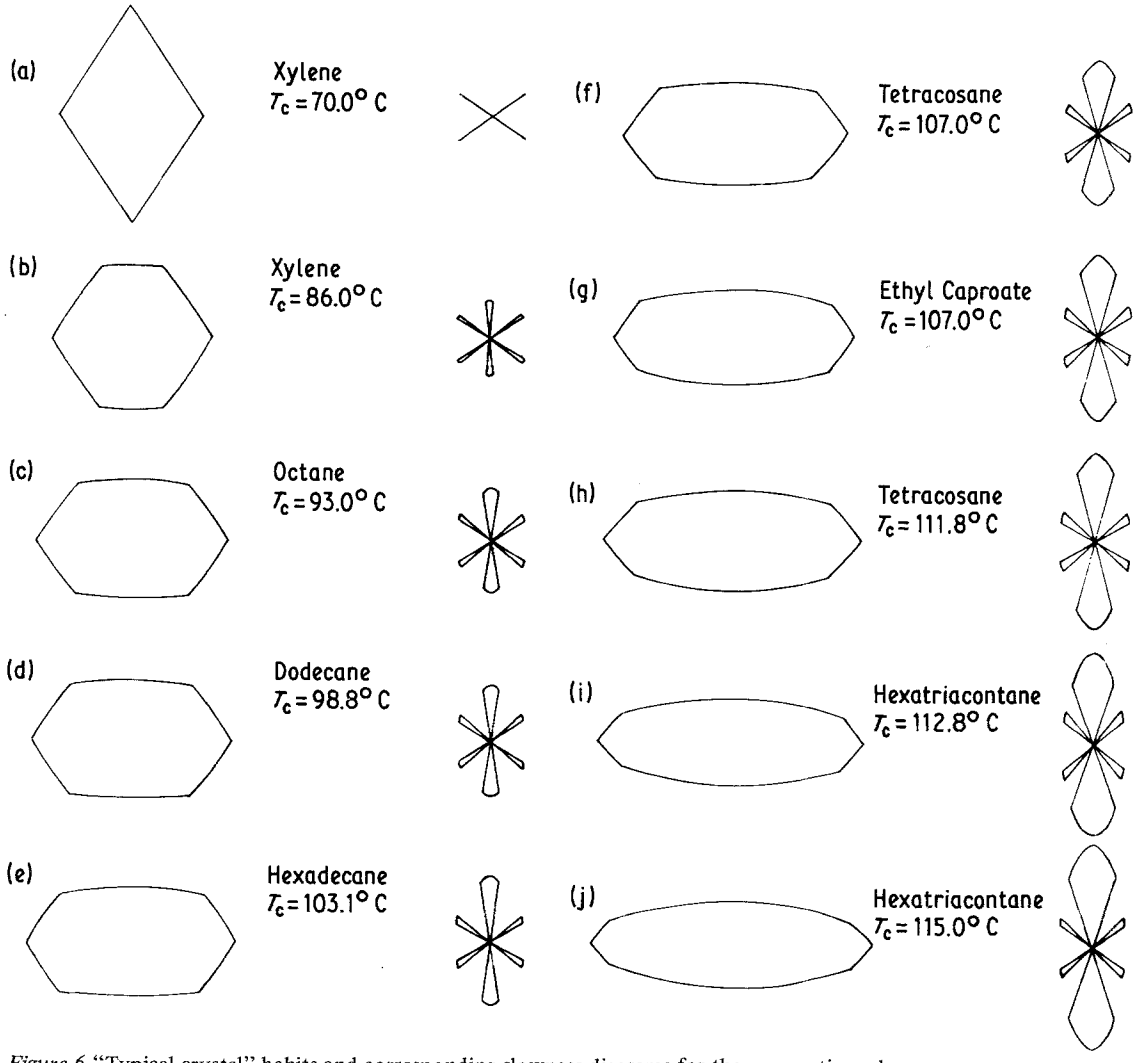

Figure 6 "Typical crystal" habits and corresponding slowness diagrams for the preparations shown.

TABLE II Parameters corresponding to the crystal morphologies illustrated in Fig. 6

Solvent	T_c (° C)	A/B	A/C	θ (°)	ϕ (°)	x/y (× 10^2)	G_{110}/G_{100}
Xylene	70.0	0.70 ± 0.05	0.70 ± 0.05	112.5 ± 2.0	112.5 ± 2.0	–	–
Xylene	86.0	1.10 ± 0.05	1.15 ± 0.05	115.0 ± 2.0	111.0 ± 2.0	3.3	1.07
Octane	93.0	1.60 ± 0.10	1.70 ± 0.10	114.5 ± 2.0	109.0 ± 1.0	3.6	1.32
Dodecane	98.8	1.70 ± 0.10	1.80 ± 0.10	114.0 ± 2.0	108.5 ± 2.0	3.2	1.40
Hexadecane	103.1	1.90 ± 0.20	2.10 ± 0.10	119.5 ± 2.0	111.0 ± 2.0	3.8	1.62
Tetracosane	107.0	2.20 ± 0.20	2.65 ± 0.20	111.5 ± 3.0	102.5 ± 1.5	5.5	1.76
Ethyl caproate	107.0	2.50 ± 0.30	3.45 ± 0.30	116.5 ± 3.0	109.0 ± 3.0	7.0	2.03
Tetracosane	111.8	2.60 ± 0.20	3.55 ± 0.25	107.0 ± 2.0	97.0 ± 2.0	6.9	2.18
Hexatriacontane	112.8	3.00 ± 0.20	4.80 ± 0.30	109.0 ± 5.0	96.5 ± 4.0	7.6	2.25
Hexatriacontane	115.0	3.25 ± 0.30	6.00 ± 1.00	115.0 ± 2.0	99.5 ± 3.0	8.3	2.53

Fig. 7 shows the variation of the minimun axial ratio, A/B, with crystallization temperature, for all the crystals for which this parameter could be measured. It was not possible to obtain values for crystals grown from hexyl acetate or dodecanol due to the prevalence of the cluster-type growth mentioned previously. For a given crystal preparation, the measured minimum and maximum axial ratios varied by typically 5–10% from a mean value. For each solvent the axial ratios increase with increasing crystallization temperature and there is also a general trend of increase in axial ratio with temperature regardless of solvent. For the more volatile solvents, notably octane and dodecane, an additional error is introduced by the fact that some evaporation of solvent occurs during crystallization at the higher temperatures. In an extreme case, up to 30% of the solvent may be lost by evaporation, and since morphology is dependent on concentration, this may affect the results. The rather high values of axial ratio for the preparations grown in octane at 99.5° C and dodecane at 103.1° C, could be due to this effect. The results may also be affected by the fact that the polymer

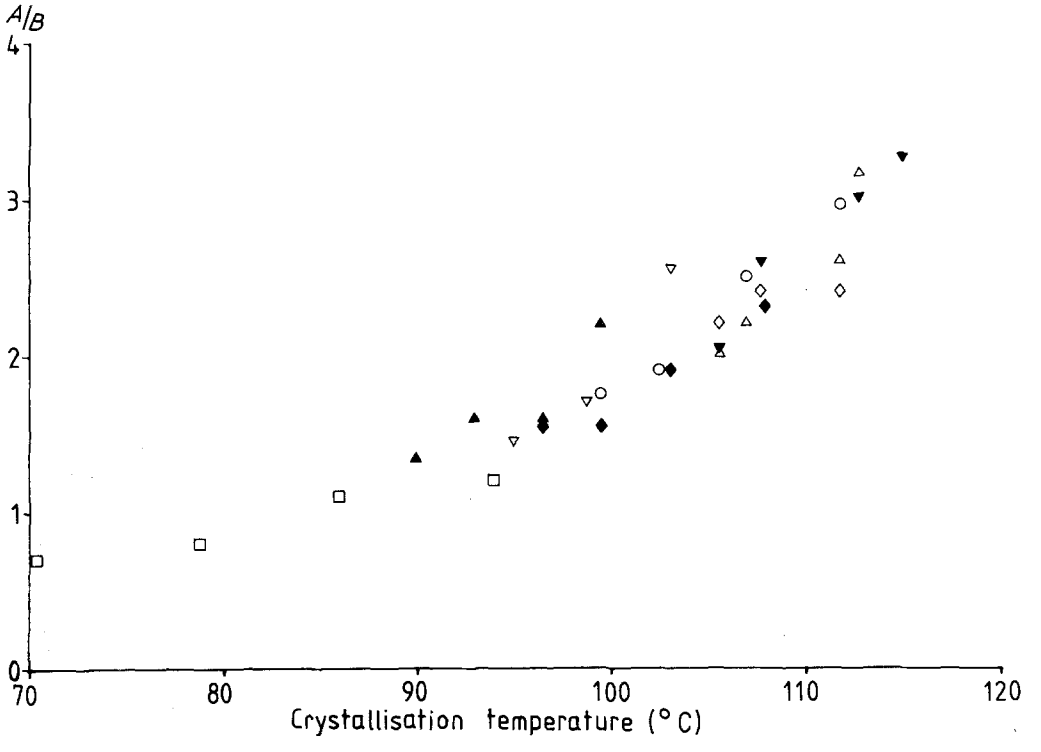

Figure 7 Variation of minimum axial ratio, A/B, with crystallization temperature. □-xylene, ▲-octane, ▽-dodecane, ♦-hexadecane, △-tetracosane, ▼-hexatriacontane, ○-ethyl esters, ◇tetradecanol.

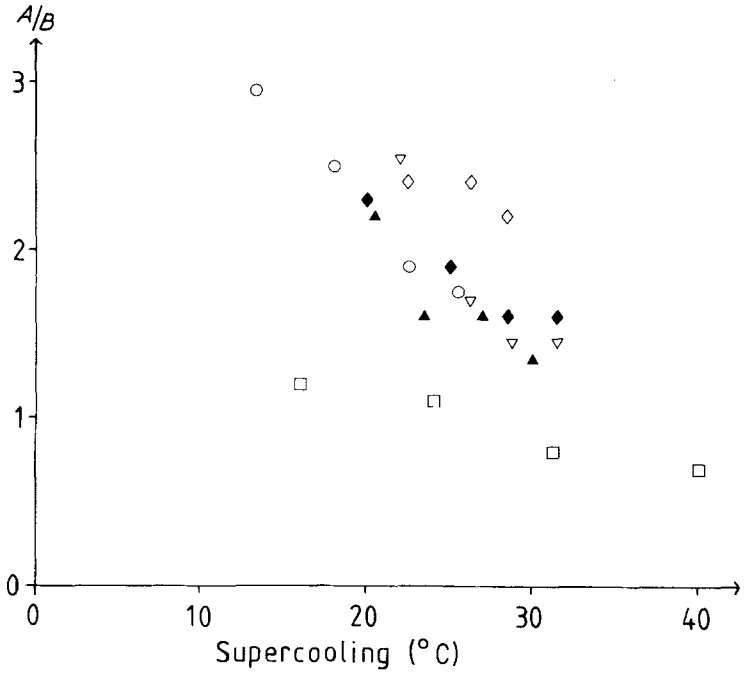

Figure 8 Variation of minimum axial ratio, A/B, with supercooling. □-xylene, ▲-octane, ▽-dodecane, ◆-hexadecane, ○-ethyl esters, ◇-tetradecanol.

used contained a fairly wide distribution of molecular weights. As the crystallization temperature is raised, the proportion of material which is capable of crystallization is reduced. Thus the concentration of crystallizable species is effectively lowered and the average molecular weight is effectively raised. Both these factors could lead to a lowered value of axial ratio. These effects are difficult to quantify and ideally the experiments should be repeated using sharp molecular weight fractions. Fig. 7 indicates in the first place that there is a correlation between axial ratio and crystallization temperature (T_c). There is also some variation with solvent for a given T_c, but this does not obscure the main trend. In Fig. 8 the axial ratios are plotted as a function of supercooling, ΔT, for a selection of solvents. The derivation of the ΔT values will be discussed in Part 3 of this series [2]. It can be seen from Fig. 8 that there is no correlation between the axial ratio and the supercooling among different classes of solvent. However, within the paraffin series, some supercooling dependence is indicated. This can be seen by studying the results for octane, dodecane and hexadecane on the two graphs. In Fig. 7 the curves for these paraffinic solvents are slightly displaced from each other along the temperature axis while in Fig. 8 they practically coincide. It would appear that there is definitely a broad correlation between axial ratio and crystallization temperature but that this is modified by a supercooling dependence within a series of similar solvents.

The curvature of the "100" faces, expressed as the ratio x/y, is given for a selection of crystals in Table II. "100" faces, where seen, were always curved to some extent, although the effect was difficult to quantify in cases where the faces were relatively short. The degree of curvature is small, and fairly constant, for crystals with axial ratios below about 2 (corresponding to crystallization temperatures of about 105° C). Above this value the curvature increases quite rapidly.

The "110" faces appear perfectly smooth at the lowest crystallization temperatures, but slight curvature can be detected as the crystallization temperature is increased. This is reflected in the difference between the extreme values of the apex angles, θ and ϕ. Measurements of θ and ϕ are complicated by the fact that the "110" faces often show discontinuities, and that the point of intersection of the "110" with the "100" faces is not always clearly defined. The actual values of θ and ϕ are rather variable, but the quantity $\theta - \phi$ increases fairly regularly as the temperature is increased, indicating that the "110" faces are

becoming more curved. This curvature is in all cases less than that of the "100" faces.

The variation in axial ratio is indicative of a gradual change in the relative growth rates of the "110" and "100" faces. This is seen as an increase in the length of the lobes corresponding to the "100" faces in the slowness diagrams given in Fig. 6. As the crystallization temperature is increased, the "100" faces grow more slowly compared to the "110" faces. The increase in curvature can be seen in the slowness diagrams as an increase in the angular spread of the lobes corresponding to the "100" faces.

7. Discussion and conclusions

For the particular crystallization conditions studied, the following conclusions can be drawn.

1. For crystals grown from a given solvent the axial ratio increases with increasing crystallization temperature.

2. Comparing crystals grown from different solvents, the axial ratio is roughly related to the crystallization temperature, although there is some solvent effect. A dependence of habit on supercooling is indicated within the paraffin series, but not between solvents of different types.

3. "100" crystal faces are usually curved and the degree of curvature increases with crystallization temperature.

4. "110" crystal faces are initially straight, but show an increasing slight curvature with increasing crystallization temperature.

5. At high temperatures the crystals tend to grow in clusters, with many crystals growing in all directions from a common centre. In some solvents this is the prevalent morphology at all crystallization temperatures.

Comparisons can be drawn between the crystal morphologies reported here and those obtained under similar conditions from the melt. The preferential growth of crystals in the *b* direction and the cluster morphology prevalent at higher crystallization temperatures show some similarities with spherulitic growth. However, even the most elongated single crystals appear to grow with constant shape, while the lamellae in spherulites grow radially outwards. More detailed investigations of the structure and growth of the single crystal clusters could provide useful information on this point. The morphology of polyethylene droplets crystallized from the melt at high supercoolings has been studied by Martinez-Salazar *et al.* [23]. A transition from well-defined growth facets to rough curved faces is seen for crystallization temperatures between 90 and 105° C, corresponding to a supercooling range of about 55–40° C. At the highest supercoolings, angles can be measured which correspond to the joining of {110} and {100} faces. For single crystals, well-defined growth facets are seen in crystals with an axial ratio of about 1 or less. As the axial ratio increases, increasing degrees of curvature are seen. If the axial ratio against supercooling curve found for the paraffin series (see Fig. 8) is assumed to apply also to crystallization from the melt then the droplet results suggest $A/B \lesssim 1$ for $\Delta T \lesssim 55°$ C and $A/B > 1$ for $\Delta T \simeq 40°$ C. These values are consistent with the solution grown single crystal results.

Single crystals grown from the melt by Labaig [24] at temperatures between 122° C and 132° C exhibited leaf-shaped morphologies, with axial ratios as high as 15. Quantitative comparisons are difficult to make due to the strong molecular weight dependence found. The general trend of increasing axial ratio with increasing crystallization temperature was seen, but there was no evidence for the existence of "110" and "100" faces, only two intersecting curved faces. Crystals of this type might be expected from solution growth at lower supercoolings than those achieved here, from an extrapolation of the data available.

The accepted model for polymer crystal growth, which was developed from studies of the lozenge and truncated lozenge morphologies first encountered, is of chains lying down in a fairly regular manner along the {110} and {100} growth faces. There is much evidence to support this view, the most striking perhaps being the existence of well-defined crystallographically distinct sectors within the crystal. For the curved crystals reported here the model obviously needs some modification. Growth no longer occurs along smooth crystallographic faces. The curvature observed implies a rough growth surface on a molecular scale, the degree of roughness increasing with crystallization temperature. Whether any degree of sectorization is retained as the crystals become more curved is not apparent, and this question will be considered further in Part 2 of this series [1].

The most successful theory of polymer crystal growth has been the kinetic theory developed mainly by Hoffman *et al.* [6]. This is a secondary nucleation theory, based on the model

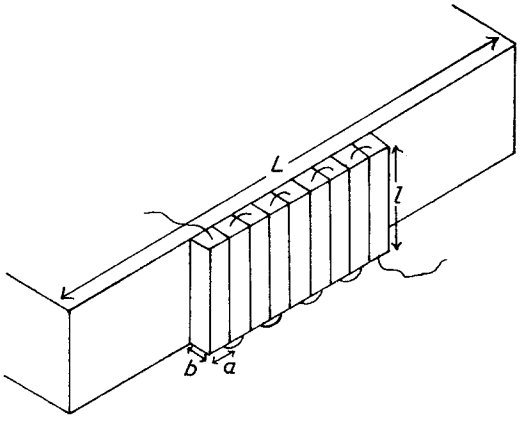

Figure 9 Model used for the kinetic theory of polymer crystallization (Hoffman *et al.* [6]). A chain segment, with the dimensions shown, attaches to a substrate of length L and spreads along the crystal face to complete a layer of thickness b.

shown in Fig. 9. It has been used successfully to account for observed values of fold length and growth rate for both solution and melt crystallization over a certain range of conditions. The work presented here provides a challenge to its applicability over a wider temperature range, where the crystals take up increasingly curved habits. Quantitative assessment of the theory will be presented in Part 3 [2]. Here it suffices to consider its ability to account for the changes in crystal shape seen experimentally. The Hoffman theory identifies three different types of growth, dependent on the relative rates of nucleation and spreading [25, 26]. These are referred to as Regimes I, II, and III. These growth regimes were established for crystallization from the melt, using growth rate data. They are also assumed to apply to solution crystallization but this is presently untested. The regime in which crystallization occurs affects the resulting molecular trajectory. Fig. 10 shows typical growth fronts for each case, and possible molecular paths. In Regime I the growth front is smooth and all folds lie parallel to the edge of the crystal. In Regime II the surface is rougher and some folds are now perpendicular to the crystal edges. Regime III also produces a rough growth front. Solution crystallization is usually assumed to fall within Regime I. It is difficult to see how the occurrence of curved morphologies at high crystallization temperatures can be accommodated into the growth regime concept of the kinetic theory. Crystals formed at lower supercoolings would be expected to grow more slowly and hence, using this model, to show well-

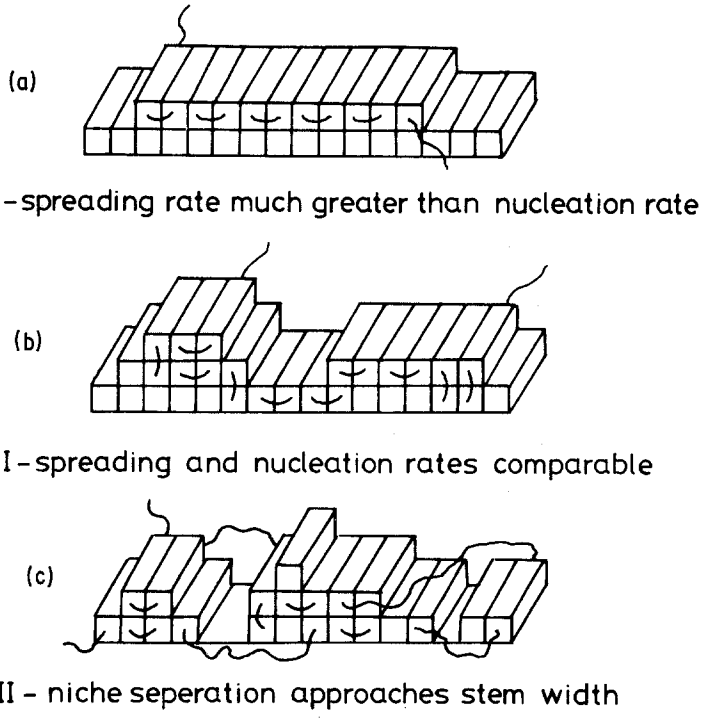

Figure 10 Typical growth fronts and molecular trajectories for (a) Regime I–spreading rate much greater than nucleation rate (b). Regime II–spreading and nucleation rates comparable. (c) Regime III–niche separation approaches stem width. By the theories of Hoffman, Regimes I, II and III pertain to increasing supercoolings respectively.

defined facets and more regular fold surface structure. The former prediction is certainly not fulfilled and there is some evidence to suggest that the latter is also questionable (see Part 2 [1]). The results imply that under conditions of low supercooling some modification to the simple model is required. Possible processes which could be involved are isothermal thickening (although the results to be presented in Part 3 [2] reveal no significant thickening at these temperatures), or surface roughening, as proposed in recent papers by Sadler [14, 27]. The surface roughening theory is as yet at an early stage of development, but provides an interesting possible explanation for the variations in lateral habit of polyethylene single crystals. Sadler applies equilibrium surface roughening theory developed for crystal growth of small molecules to the case of polyethylene. Surface roughness will occur if the binding energy between units in a crystal, ϵ, is comparable with kT, where k is the Boltzmann constant and T is the absolute temperature. As the crystallization temperature is increased, a transition would be expected between nucleation controlled growth onto smooth surfaces, and continuous nucleation free growth onto a rough surface. A transition temperature, T_R, can be defined, and theoretical calculations suggest that this occurs where $kT_R/\epsilon \simeq 0.63$. Such transitions have been seen in some inorganic systems [28].

The observation of curved crystal morphologies in polyethylene is indicative of an atomically rough growth surface structure, so the applicability of roughening theory to this system should be considered. The observed trend in crystal shape with increasing crystallization temperature could be understood by making the assumption that nominal "100" faces are always rough, while the "110" faces undergo a transition from a smooth to a fairly rough surface with increasing temperature. As the crystallization temperature is raised above this transition temperature, roughness of the "110" faces, and hence their growth rate relative to the "100" faces, increases. This difference in behaviour between the two types of face could be explained by the difference in the relative binding energies between molecules. Since the interstem distance is higher along ⟨010⟩ than ⟨110⟩, ϵ_1 would be expected to be smaller, and thus T_R lower, for the "100" faces.

At this early stage in its development the theory has many limitations, but it provides an interesting possible extension to the kinetic theory and its success in explaining morphological variations suggests that surface roughening may indeed be a relevant factor in discussing polymer crystallization.

In conclusion, polyethylene crystals have been grown from solution at temperatures which attain and exceed those commonly used for crystallization from the melt. Thus a long outstanding overlap has been established between solution and melt growth both in terms of absolute crystallization temperature and supercooling, allowing the two to be compared with respect to common points of reference. As a first step, the present paper has characterized the lateral habit features of the crystals. The new qualitative feature of curved crystal faces, recognized earlier [12, 13], has been systematically examined and shows correlation with corresponding features seen at similar temperatures in the melt. More significantly, the implications of these observations for some basic issues of polymer crystallization have been recognized. The results highlight the need for a re-appraisal of the range of applicability of the existing theories and provide some potential justification for some novel approaches. The continued exploitation of the newly accessible crystallization regimes, comprising three-dimensional morphology, fold length and related issues, will follow in the subsequent parts of the series.

References

1. S. J. ORGAN and A. KELLER, *J. Mater. Sci.* **20** (1985).
2. *Idem, ibid.* **20** (1985).
3. J. MARTINEZ-SALAZAR, P. J. BARHAM, and A. KELLER, *ibid.* **20** (1985).
4. P. J. BARHAM, R. A. CHIVERS, A. KELLER, J. MARTINEZ-SALAZAR and S. J. ORGAN, *ibid.* **20** (1985).
5. A. KELLER, *Rep. Prog. Phys.* **31** (1968) 623.
6. J. D. HOFFMAN, G. T. DAVIS and J. I. LAURITZEN in "Treatise on Solid State Chemistry" Vol. 3, edited by Hannay (Plenum Press, New York 1976) pp. 497–614.
7. J. D. HOFFMAN and J. J. WEEKS, *J. Chem. Phys.* **42** (1965) 4301.
8. J. RAULT, *J. Macromol. Sci.* **B15** (1978) 567.
9. P. J. BARHAM, R. A. CHIVERS, D. A. JARVIS, J. MARTINEZ-SALAZAR and A. KELLER, *J. Polym. Sci. Polym. Lett. Ed.* **19** (1981) 539.
10. R. A. CHIVERS, J. MARTINEZ-SALAZAR, P. J. BARHAM and A. KELLER, *ibid.* **20** (1982) 1717.
11. P. J. BARHAM, D. A. JARVIS and A. KELLER, *ibid.* **20** (1982) 1733.
12. H. D. KEITH, *J. Appl. Phys.* **35** (1964) 3115.
13. F. KHOURY and L. H. BOLZ, 38th Annual Proceedings of the Electron Microscopy Society of

America" San Francisco, California. (1980) edited by G. W. Bailey.
14. D. M. SADLER, *Polym.* **24** (1983) 1401.
15. D. C. BASSETT, F. C. FRANK and A. KELLER, *Phil. Mag.* 8 1753.
16. T. KAWAI and A. KELLER, *ibid.* **11** (1965) 1165.
17. A. NAKAJIMA, F. HAMADA, S. HAYASHI and T. SUMIDA, *Kolloid-Z.Z. Polym.* **222** (1968) 10.
18. D. J. BLUNDELL, A. KELLER and A. J. KOVACS, *Polym. Lett.* **4** (1966) 481.
19. A. KELLER, *J. Polym. Sci.* **36** (1959) 369.
20. D. T. GRUBB, A. KELLER and G. W. GROVES, *J. Mater. Sci.* 7 (1972) 131.
21. F. C. FRANK in "Growth and Perfections of Crystals" edited by R. H. Doremus, B. W. Roberts and D. Turnbull (Chapman and Hall, London 1958) pp. 411–9.
22. D. J. BLUNDELL and A. KELLER, *J. Macromol. Sci.* **B2** (1968) 337.
23. J. MARTINEZ-SALAZAR, P. J. BARHAM and A. KELLER, *J. Polym. Sci. Polym. Phys. Ed.* **22** (1984) 1085.
24. J. J. LABAIG, PhD Thesis, University of Strasbourg (1978).
25. J. I. LAURITZEN and J. D. HOFFMAN, *J. Appl. Phys.* **44** (1973) 4340.
26. J. D. HOFFMAN, *Polym.* **24** (1983) 3.
27. D. M. SADLER and G. H. GILMER, *Polymer* **25** (1984) 1446.
28. K. A. JACKSON in "Crystal Growth", (Pergamon Press, Oxford 1967). p. 17.

Received 15 August
and accepted 13 September 1984